

Effects of magnesium substitution on the magnetic properties of $\text{Nd}_{0.7}\text{Sr}_{0.3}\text{MnO}_3$

M. Tseggai^{a,*}, R. Mathieu^a, P. Nordblad^a, R. Tellgren^a, L.V. Bau^b, D.N.H. Nam^b, N.X. Phuc^b, N.V. Khiem^c, G. André^d, F. Bourée^d

^aThe Ångström Laboratory, Department of Engineering Sciences, Uppsala University, Solid State Physics, Room 4340, Box 534, SE-751 21 Uppsala, Sweden

^bInstitute of Materials Science, VAST, Nghiado-Caugiay-Hanoi, Vietnam

^cDepartment of Science and Technology, Hongduc University, Thanhhoa, Vietnam

^dLaboratoire Léon Brillouin, CEA/Saclay, F-91 191 Gif sur Yvette, France

Received 13 August 2004; received in revised form 13 January 2005; accepted 20 January 2005

Abstract

Effects of magnesium substitution on the magnetic properties of $\text{Nd}_{0.7}\text{Sr}_{0.3}\text{MnO}_3$ have been investigated by neutron powder diffraction and magnetization measurements on polycrystalline samples of composition $\text{Nd}_{0.7}\text{Sr}_{0.3}\text{MnO}_3$, $\text{Nd}_{0.6}\text{Mg}_{0.1}\text{Sr}_{0.3}\text{MnO}_3$, $\text{Nd}_{0.6}\text{Mg}_{0.1}\text{Sr}_{0.3}\text{Mn}_{0.9}\text{Mg}_{0.1}\text{O}_3$, and $\text{Nd}_{0.6}\text{Mg}_{0.1}\text{Sr}_{0.3}\text{Mn}_{0.8}\text{Mg}_{0.2}\text{O}_3$. The pristine compound $\text{Nd}_{0.7}\text{Sr}_{0.3}\text{MnO}_3$ is ferromagnetic with a transition temperature occurring at about 210 K. Increasing the Mg-substitution causes weakened ferromagnetic interaction and a great reduction in the magnetic moment of Mn. The Rietveld analyses of the neutron powder diffraction (NPD) data at 1.5 K for the samples with Mg concentration, $y = 0.0$ and 0.1 , show ferromagnetic Mn moments of $3.44(4)$ and $3.14(4) \mu_B$, respectively, which order along the [001] direction. Below 20 K the Mn moments of these samples become canted giving an antiferromagnetic component along the [010] direction of about $0.4 \mu_B$ at 1.5 K. The analyses also show ferromagnetic polarization along [001] of the Nd moments below 50 K, with a magnitude of almost $1 \mu_B$ at 1.5 K for both samples. In the samples with Mg substitution of 0.2 and 0.3 only short range magnetic order occurs and the magnitude of the ferromagnetic Mn moments is about $1.6 \mu_B$ at 1.5 K for both samples. Furthermore, the low-temperature NPD patterns show an additional very broad and diffuse feature resulting from short range antiferromagnetic ordering of the Nd moments.

© 2005 Elsevier Inc. All rights reserved.

Keywords: (Perovskite) manganites; Neutron powder diffraction; Magnesium substitution; Magnetic moment; Ferromagnetic; Transition temperature; Antiferromagnetic

1. Introduction

Magnetic and transport properties of the hole-doped manganese oxides of perovskite-type structure, $R_{1-x}D_x\text{MnO}_3$ ($R = \text{La}^{3+}$, Pr^{3+} , Nd^{3+} , ...; $D = \text{Ca}^{2+}$, Sr^{2+} , Ba^{2+} , and Pb^{2+}), were first studied already in the 1950s [1–4]. A revived interest in the manganites occurred after the discovery of the colossal magnetoresistance (CMR) effect [5,6] in the materials. Partial

substitution of the trivalent rare earth R^{3+} with a divalent D^{2+} causes a corresponding amount of Mn^{3+} to be converted to Mn^{4+} and in this way a mixed valence state is introduced in the materials [1,2]. In this state, Mn^{3+} and Mn^{4+} have the electronic configuration $t_{2g}^3 \cdot e_g^1$ ($S = 2$) and t_{2g}^3 ($S = 3/2$), respectively.

The CMR and the ferromagnetic properties of manganites are described by double exchange (DE) interaction involving the overlapping of the manganese d and oxygen p orbitals and are hence greatly influenced by small variations of the Mn–Mn distance and the Mn–O–Mn bond angle [7]. Changing the content of D

*Corresponding author. Fax: +46 0 18 50 01 31.

E-mail address: mehreteab.tseggai@angstrom.uu.se (M. Tseggai).

substitution from the CMR composition $x = 0.3$ dramatically affects the (DE) interaction in the manganites. The *A*-site substitution influences the magnetic properties and the CMR by tuning the $\text{Mn}^{3+}/\text{Mn}^{4+}$ ratio and changing the Mn–Mn distance and the Mn–O–Mn bond angle [8–10]. Similar effects are also obtained by substituting Mn with other transition metal cations such as Fe^{3+} , Co^{3+} , Cr^{3+} , Cu^{2+} , or with other metal ions such as Al^{3+} , Ga^{3+} , In^{3+} , Sn^{4+} [11–14].

$\text{Nd}_{0.7}\text{Sr}_{0.3}\text{MnO}_3$ is an insulating paramagnet above T_C and a metallic ferromagnet below T_C . In a rather narrow range of doping levels near $x = 0.3$, the DE mechanism [1] qualitatively describes the metallic ferromagnetic phase of $\text{Nd}_{0.7}\text{Sr}_{0.3}\text{MnO}_3$. The strength of DE interaction can be changed in different ways e.g.: By controlling the $\text{Mn}^{3+}/\text{Mn}^{4+}$ ratio by varying the x -value or by changing the average *A*-site cation radius $\langle r_A \rangle$ keeping the $\text{Mn}^{3+}/\text{Mn}^{4+}$ ratio fixed at 7/3 [9,15]. Magnetic and transport properties of $\text{Nd}_{0.7}\text{Sr}_{0.3}\text{MnO}_3$ substituted with Mg have been investigated by Nam et al. [16]. They found that Mg-substitution changed the physical properties of $\text{Nd}_{0.7}\text{Sr}_{0.3}\text{Mn}_{1-y}\text{Mg}_y\text{O}_3$ ($y = 0, 0.03, 0.06, 0.1, 0.2, \text{ and } 0.3$) from a low-temperature metallic ferromagnet to an insulating system with spin glass characteristics for $y \geq 0.2$.

The effects of Mg substitution on the crystallographic structure of $\text{Nd}_{0.7}\text{Sr}_{0.3}\text{MnO}_3$ have recently been studied by Tseggai et al. [17]. It was found that for samples of nominal composition $\text{Nd}_{0.7}\text{Sr}_{0.3}\text{Mn}_{1-y}\text{Mg}_y\text{O}_3$, magnesium in fact substituted neodymium (on the *A*-site) rather than manganese for contents up to $y = 0.1$ (y is the concentration of Mg substitution). For $y > 0.1$, the Nd-site appeared saturated and Mg started to substitute for Mn on the *B*-site. Moreover, the magnesium substituted samples showed a slight structural distortion and decrease in the unit cell volume with respect to the pristine compound.

In this paper, the effects of Mg substitution on the magnetic properties of $\text{Nd}_{0.7}\text{Sr}_{0.3}\text{MnO}_3$ are investigated by neutron powder diffraction and magnetization measurements on the same samples as in Ref. [17].

2. Experiments

Polycrystalline samples of composition $\text{Nd}_{0.7}\text{Sr}_{0.3}\text{Mn}_{1-y}\text{Mg}_y\text{O}_3$ ($y = 0, 0.1, 0.2, \text{ and } 0.3$) have been prepared by the standard solid-state reaction method. Details of the sample preparation are described in Ref. [17]. All samples were examined by X-ray and neutron powder diffraction and found to be pure single-phased with orthorhombic symmetry and space group *Pnma* (No. 62, $z = 4$). However, as mentioned above, chemical analyses and neutron diffraction results [17] revealed that the actual composition of the Mg-doped samples was $\text{Nd}_{0.6}\text{Mg}_{0.1}\text{Sr}_{0.3}\text{MnO}_3$, $\text{Nd}_{0.6}\text{Mg}_{0.1}\text{Sr}_{0.3}$

$\text{Mn}_{0.9}\text{Mg}_{0.1}\text{O}_3$ and $\text{Nd}_{0.6}\text{Mg}_{0.1}\text{Sr}_{0.3}\text{Mn}_{0.8}\text{Mg}_{0.2}\text{O}_3$, respectively.

Neutron powder diffraction data were recorded at Laboratoire Léon Brillouin, CEA, Saclay on the 2-axis powder diffractometer G 4-1 using a neutron wavelength of $\lambda = 2.4300 \text{ \AA}$. The diffractograms were recorded at several temperatures between 1.5 and 250 K over the angular range $11^\circ \leq 2\theta \leq 90.9^\circ$ with step size 0.1° in 2θ .

Chemical analyses of the samples were made using an inductively coupled plasma atomic emission spectrometer (ICP-AES), Spectroflame P, Kleve, Germany.

The magnetization measurements were performed on a Quantum Design MPMS XL SQUID magnetometer. In these measurements, magnetization as a function of temperature data was collected in the temperature range 10–300 K in an applied field of 20 Oe, and isothermal magnetization at low temperature (10 K) were performed up to a field of 50 kOe.

3. Results

3.1. Sample composition

The crystallographic characterization of the investigated samples has been described earlier in Ref. [17]. The results from the chemical analyses of the samples (in weight%) are detailed in Table 1, showing the measured composition of each sample (meas) together with the corresponding calculated data for the intended composition of the samples (intend) and the values expected from the actual composition of the samples derived from the refinements of the neutron data (NDres) of Ref. [17]. Some caution has to be taken when interpreting these results. Apart from rather large systematic and absolute errors in the chemical analyses, e.g., since the oxygen

Table 1
Compositions of the samples according to the chemical analyses (meas): all values are given in wt% of the dried material. Also shown are calculated values for the intended (intend) composition and the actual compositions derived from the neutron diffraction data (NDres)

Sample	Label	Nd (wt%)	Sr (wt%)	Mn (wt%)	Mg (wt%)
$y = 0$	Meas	45.0	12.1	25.2	0
	Intend	43.8	11.5	23.9	0
	NDres	43.8	11.5	23.9	0
$y = 0.1$	Meas	43.7	12.9	24.9	0.6
	Intend	44.4	11.6	21.8	1.1
	NDres	39.6	12.1	25.2	1.1
$y = 0.2$	Meas	44.0	12.8	21.5	1.3
	Intend	45.0	11.8	19.6	2.1
	NDres	40.2	12.3	23.0	2.2
$y = 0.3$	Meas	43.7	12.6	18.9	2.0
	Intend	45.6	12.0	17.4	3.3
	NDres	40.8	12.5	20.8	3.4

content cannot be directly determined by the method used; the neutron analyses only concern the main phase (the phase of interest in our study), whereas the chemical analyses also include contributions from any remaining impurities in the samples (not resolved by the X-ray or neutron diffractograms). However, looking at the results from the chemical analysis in the light of its intrinsic uncertainty, there is a clear indication that going from sample $y = 0$ to 0.1, the Nd content is lower and the Mn content higher than expected from the intended composition. Increasing the Mg content further, yield compositions of the samples $y = 0.2$ and 0.3 that follow the trends of the intended composition change—a closely constant Nd and a decreasing Mn content. This information was used as input to our Rietveld refinements of the room temperature neutron diffractograms, allowing substitution of Mg for Nd as well as for Mn. It was however found that the quality of the refinements

was quite insensitive to allowing small amounts of oxygen deficiency; therefore, full oxygen occupancy has been used for all samples in the final refinements. The results from these refinements as to the occupancy of the different crystallographic positions are given in Table 2 together with magnetic data.

3.2. Magnetization measurements

The magnetic response of the samples was studied by zero-field cooled (ZFC) and field cooled (FC) magnetization measurements. In this measurement procedure, the sample is first cooled in zero-field to a low temperature where the magnetic field is applied and the ZFC magnetization recorded on heating to a high temperature above any magnetic transitions in the system. The FC magnetization is then recorded while cooling the sample down to the start temperature of the

Table 2

Nuclear and magnetic structural parameters for all the samples at 1.5 K derived from the Rietveld refinement analyses of the neutron powder diffraction data: the atomic coordinates (Å), thermal parameter (BISO), occupancies (OCC), magnetic structure (MS), magnetic moments, lattice parameters and reliability R factors are indicated. In the magnetic structure (MS) column, F and A denote ferromagnetic and A -type antiferromagnetic structures, respectively

Atom	x	y	z	BISO	OCC	T/K	MS	M_x/μ_B	M_y/μ_B	M_z/μ_B	M/μ_B
Nd_{0.7}Sr_{0.3}MnO₃											
Nd	0.027(2)	1/4	−0.001(4)	0.60(2)	0.35	1.5	F			0.90(5)	0.90(5)
Sr	0.027(2)	1/4	−0.001(4)	0.60(2)	0.15						
Mn	0	0	1/2	0.45(2)	0.50		F A			3.43(4)	3.45(5)
O1	0.491(3)	1/4	0.073(4)	0.97(1)	0.50						
O2	0.276(4)	0.030(2)	0.719(4)	0.97(1)	1.00				0.42(5)		
$a = 5.480(1) \text{ \AA}, b = 7.741(1) \text{ \AA}, c = 5.4803(6) \text{ \AA}; R_p = 5.09\%, R_{wp} = 6.96\%, R_B = 2.74\%, R_M = 2.13\%$											
Nd	0.026(2)	1/4	−0.001(4)	0.60(2)	0.35	20	F			0.22(5)	0.22(5)
Sr	0.026(2)	1/4	−0.001(4)	0.60(2)	0.15						
Mn	0	0	1/2	0.65(2)	0.50		F			3.43(4)	3.43(5)
O1	0.492(3)	1/4	0.078(3)	0.97(1)	0.50						
O2	0.272(5)	0.03(1)	0.717(3)	0.97(1)	1.00						
$a = 5.479(1) \text{ \AA}, b = 7.740(1) \text{ \AA}, c = 5.4801(6) \text{ \AA}; R_p = 5.21\%, R_{wp} = 7.15\%, R_B = 3.07\%, R_M = 1.12\%$											
Nd	0.025(2)	1/4	0.005(4)	0.86(2)	0.35	200					
Sr	0.025(2)	1/4	0.005(4)	0.86(2)	0.15						
Mn	0	0	1/2	0.65(2)	0.50		F			0.8(1)	0.8(1)
O1	0.490(3)	1/4	0.070(3)	1.38(1)	0.50						
O2	0.278(5)	0.033(2)	0.721(4)	1.38(1)	1.00						
$a = 5.486(1) \text{ \AA}, b = 7.742(1) \text{ \AA}, c = 5.4871(7) \text{ \AA}, R_p = 5.09\%, R_{wp} = 6.77\%, R_B = 3.74\%, R_M = 7.09\%$											
Nd_{0.6}Mg_{0.1}Sr_{0.3}MnO₃											
Nd	0.023(2)	1/4	0.014(3)	0.49(2)	0.30	1.5	F			0.79(6)	0.79(6)
Sr	0.023(2)	1/4	0.014(3)	0.49(2)	0.15						
Mg	0.023(2)	1/4	0.014(3)	0.49(2)	0.05						
Mn	0	0	1/2	0.68(4)	0.05		F A			3.12(4)	3.15(5)
O1	0.492(4)	1/4	0.060(4)	0.93(2)	0.50						
O2	0.278(5)	0.033(2)	0.714(4)	0.93(2)	1.00				0.43(5)		
$a = 5.457(1) \text{ \AA}, b = 7.713(1) \text{ \AA}, c = 5.4610(7) \text{ \AA}; R_p = 5.05\%, R_{wp} = 6.77\%, R_B = 3.74\%, R_M = 7.09\%$											
Nd	0.017(2)	1/4	0.013(5)	0.49(2)	0.30	29	F			0.11(6)	0.11(6)
Sr	0.017(2)	1/4	0.013(5)	0.49(2)	0.15						
Mg	0.017(2)	1/4	0.013(5)	0.49(2)	0.05						
Mn	0	0	1/2	0.68(4)	0.05		F			3.10(4)	3.10(4)

Table 2 (continued)

Atom	<i>x</i>	<i>y</i>	<i>z</i>	BISO	OCC	<i>T</i> /K	MS	<i>M_x</i> /μ _B	<i>M_y</i> /μ _B	<i>M_z</i> /μ _B	<i>M</i> /μ _B
O1	0.491(5)	1/4	0.042(5)	0.93(2)	0.50						
O2	0.283(5)	0.040(1)	0.718(5)	0.93(2)	1.00						
<i>a</i> = 5.456(1) Å, <i>b</i> = 7.712(1) Å, <i>c</i> = 5.460(1) Å; <i>R_p</i> = 5.30%, <i>R_{wp}</i> = 7.06%, <i>R_B</i> = 3.78%, <i>R_M</i> = 3.78%											
Nd	0.021(3)	1/4	0.018(3)	0.49(2)	0.30	200	F			0	0
Sr	0.021(3)	1/4	0.018(3)	0.49(2)	0.15						
Mg	0.021(3)	1/4	0.018(3)	0.49(2)	0.05						
Mn	0	0	1/2	0.68(4)	0.05		F			0	0
O1	0.494(5)	1/4	0.059(6)	0.93(2)	0.50						
O2	0.274(6)	0.033(21)	0.712(4)	0.93(2)	1.00						
<i>a</i> = 5.455(1) Å, <i>b</i> = 7.707(1) Å, <i>c</i> = 5.4573(7) Å; <i>R_p</i> = 5.64%, <i>R_{wp}</i> = 7.24%, <i>R_B</i> = 5.32%											
Nd _{0.6} Mg _{0.1} Sr _{0.3} Mn _{0.9} Mg _{0.1} O ₃											
Nd	0.028(1)	1/4	−0.001(2)	0.44(2)	0.30	1.5	A	1.9(1)			1.9(1)
Sr	0.028(1)	1/4	−0.001(2)	0.44(2)	0.15						
Mg	0.028(1)	1/4	−0.001(2)	0.44(2)	0.05						
Mn	0	0	1/2	0.49(4)	0.45		F			1.66(3)	1.66(3)
Mg	0	0	1/2	0.49(4)	0.05						
O1	0.490(2)	1/4	0.074(2)	1.00(2)	0.50						
O2	0.273(3)	0.0281(8)	0.719(2)	1.00(2)	1.00						
<i>a</i> = 5.4561(4) Å, <i>b</i> = 7.7068(5) Å, <i>c</i> = 5.4618(4) Å; <i>R_p</i> = 3.10%, <i>R_{wp}</i> = 3.91%, <i>R_B</i> = 2.14%, <i>R_M</i> = 2.67%											
Nd	0.028(1)	1/4	−0.004(2)	0.44(2)	0.30	20	A	1.7(1)			1.7(1)
Sr	0.028(1)	1/4	−0.004(2)	0.44(2)	0.15						
Mg	0.028(1)	1/4	−0.004(2)	0.44(2)	0.05						
Mn	0	0	1/2	0.49(4)	0.45		F			1.59(4)	1.59(4)
Mg	0	0	1/2	0.49(4)	0.05						
O1	0.492(2)	1/4	0.079(2)	1.00(2)	0.50						
O2	0.274(3)	0.0252(9)	0.719(3)	1.00(2)	1.00						
<i>a</i> = 5.4670(4) Å, <i>b</i> = 7.7141(5) Å, <i>c</i> = 5.4655(4) Å; <i>R_p</i> = 3.43%, <i>R_{wp}</i> = 4.37%, <i>R_B</i> = 2.23%, <i>R_M</i> = 4.38%											
Nd	0.028(1)	1/4	−0.005(2)	0.44(2)	0.30	100	A	0			0
Sr	0.028(1)	1/4	−0.005(2)	0.44(2)	0.15						
Mg	0.028(1)	1/4	−0.005(2)	0.44(2)	0.05						
Mn	0	0	1/2	0.49(4)	0.45		F			1.21(6)	1.21(6)
Mg	0	0	1/2	0.49(4)	0.05						
O1	0.493(2)	1/4	0.081(2)	1.00(2)	0.50						
O2	0.274(3)	0.025(1)	0.720(3)	1.00(2)	1.00						
<i>a</i> = 5.4734(5) Å, <i>b</i> = 7.7193(5) Å, <i>c</i> = 5.4693(4) Å; <i>R_p</i> = 3.71%, <i>R_{wp}</i> = 4.54%, <i>R_B</i> = 2.75%, <i>R_M</i> = 8.91%											
Nd _{0.6} Mg _{0.1} Sr _{0.3} Mn _{0.8} Mg _{0.2} O ₃											
Nd	0.026(1)	1/4	−0.007(1)	0.34(2)	0.30	1.5	A	1.6(1)			1.6(1)
Sr	0.026(1)	1/4	−0.007(1)	0.34(2)	0.15						
Mg	0.026(1)	1/4	−0.007(1)	0.34(2)	0.05						
Mn	0	0	1/2	0.44(5)	0.40		F			1.65(4)	1.65(4)
Mg	0	0	1/2	0.44(5)	0.10						
O1	0.482(2)	1/4	0.059(1)	0.97(2)	0.50						
O2	0.279(1)	0.0367(7)	0.719(1)	0.97(2)	1.00						
<i>a</i> = 5.4607(5) Å, <i>b</i> = 7.7145(8) Å, <i>c</i> = 5.4798(5) Å; <i>R_p</i> = 2.52%, <i>R_{wp}</i> = 3.28%, <i>R_B</i> = 3.34%, <i>R_M</i> = 7.79%											
Nd	0.025(1)	1/4	−0.008(2)	0.34(2)	0.30	20	A	1.4(1)			1.4(1)
Sr	0.025(1)	1/4	−0.008(2)	0.34(2)	0.15						
Mg	0.025(1)	1/4	−0.008(2)	0.34(2)	0.05						
Mn	0	0	1/2	0.44(5)	0.40		F			1.55(5)	1.55(5)
Mg	0	0	1/2	0.44(5)	0.10						
O1	0.484(2)	1/4	0.059(2)	0.97(2)	0.50						
O2	0.276(2)	0.0367(9)	0.713(1)	0.97(2)	1.00						
<i>a</i> = 5.4612(6) Å, <i>b</i> = 7.713(1) Å, <i>c</i> = 5.4801(6) Å; <i>R_p</i> = 3.00%, <i>R_{wp}</i> = 3.82%, <i>R_B</i> = 3.27%, <i>R_M</i> = 9.01%											
Nd	0.028(2)	1/4	−0.009(2)	0.34(2)	0.30	120	A	0			0
Sr	0.028(2)	1/4	−0.009(2)	0.34(2)	0.15						
Mg	0.028(2)	1/4	−0.009(2)	0.34(2)	0.05						
Mn	0	0	1/2	0.44(5)	0.40		F			1.32(6)	1.32(6)
Mg	0	0	1/2	0.44(5)	0.10						
O1	0.483(3)	1/4	0.060(2)	0.97(2)	0.50						
O2	0.273(3)	0.0367(1)	0.715(2)	0.97(2)	1.00						
<i>a</i> = 5.4606(8) Å, <i>b</i> = 7.714(1) Å, <i>c</i> = 5.4811(7) Å; <i>R_p</i> = 3.20%, <i>R_{wp}</i> = 4.06%, <i>R_B</i> = 3.40%, <i>R_M</i> = 2.54%											

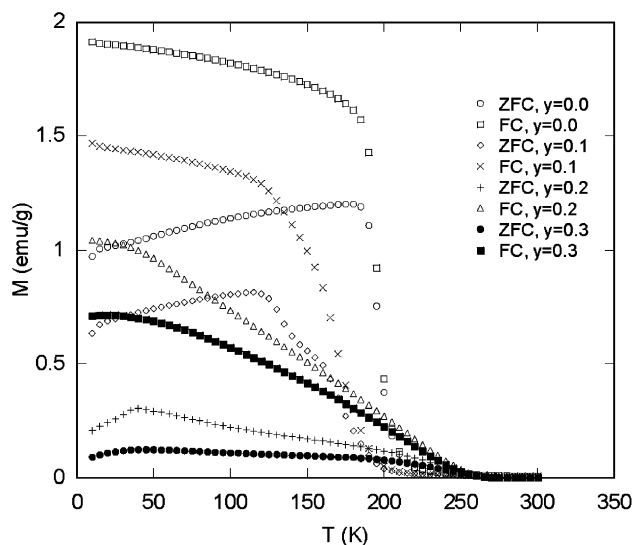


Fig. 1. Zero-field cooled (ZFC) and field cooled (FC) magnetization curves of the different samples in an applied field of 20 Oe.

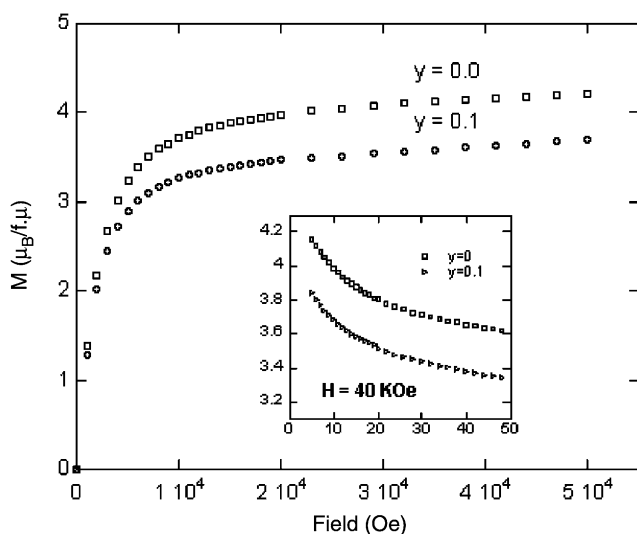


Fig. 2. Magnetization vs. magnetic field curves at 5 K for the $y = 0.0$ and 0.1 samples. The inset shows the low-temperature variation of the magnetization of these two samples in an applied field of 40 kOe.

ZFC measurement. In Fig. 1, the resulting ZFC and FC magnetization curves in an applied field of 20 Oe are shown. The samples with lower Mg concentration, $y = 0.0$ and 0.1, show ferromagnetic behaviour with transition temperatures of 210 and 180 K, respectively, however with a significant broadening for the $y = 0.1$ sample (Fig. 1). The two samples with higher Mg concentration, $y = 0.2$ and 0.3, show a more complex magnetic behaviour, with indications of a short range magnetic order already at a temperature of about 250 K and a maximum in the ZFC magnetization at low temperatures that indicates a spin glass-like order [16].

Fig. 2 shows magnetization versus field curves for the two ferromagnetic samples at 5 K. The magnetization

value at 5 T gives a magnetic moment of $4.2 \mu_B/\text{Mn}$ for $y = 0.0$ and $3.7 \mu_B/\text{Mn}$ for $y = 0.1$, assuming that only Mn contributes to the magnetization and that the ordering is ferromagnetic. However, in the inset to Fig. 2, the temperature dependence of the magnetization in an applied field of 4 T is shown in the range 0–50 K. The upturn of the magnetization and high saturation magnetization at low temperatures is due to a ferromagnetic polarization of Nd as evidenced from the analyses of the neutron diffraction data (see below).

3.3. Neutron powder diffraction (NPD)

The neutron powder diffraction data was refined by the Rietveld method using the computer program FullProf [18]. The neutron scattering lengths used were Nd = 7.69, Sr = 7.02, Mn = -3.73 , Mg = 5.375 and O = 5.803 fm. The magnetic form factors were those from the FullProf program. The total number of reflexions was 44. In carrying out the Rietveld refinement of the data, the values of the occupancies have been fixed to the values found at room temperature [17]. The values of the thermal parameters, which are difficult to refine when only low angle data is available, have been fixed at 30% of the room temperature values for temperatures below 170 K and fixed at the room temperature values for all temperatures above 170 K.

Fig. 3(a) shows the neutron powder diffraction intensities for $\text{Nd}_{0.6}\text{Mg}_{0.1}\text{Sr}_{0.3}\text{MnO}_3$ at some different temperatures, from which the additional ferromagnetic contribution for the nuclear peaks can be followed, and Fig. 3(b) shows the intensities of all compositions at 1.5 K and it clearly shows the effect of Mg substitution on magnetic properties of the materials.

Figs. 4(a) and (b) show Rietveld refinement plots of the NPD data of the samples with magnesium concentration, $y = 0.1$ and 0.2, respectively, at 1.5 K.

The refined nuclear and magnetic structural parameters at different temperatures and the associated reliability factors R_p , R_{wp} , R_B , and R_M (R_M —magnetic R -factor) are listed in Table 2. The temperature dependence of the magnetic moments for $\text{Nd}_{0.7}\text{Sr}_{0.3}\text{MnO}_3$ and $\text{Nd}_{0.6}\text{Mg}_{0.1}\text{Sr}_{0.3}\text{MnO}_3$ are shown in Fig. 5. The derived crystallographic and magnetic structures are illustrated in Fig. 6.

3.3.1. $\text{Nd}_{0.7}\text{Sr}_{0.3}\text{MnO}_3$ and $\text{Nd}_{0.6}\text{Mg}_{0.1}\text{Sr}_{0.3}\text{MnO}_3$

The magnetic moment of manganese, in the pristine compound, orders ferromagnetically along [001] below 225 K. The magnitude of the ferromagnetic component is $3.43(4) \mu_B$ at 1.5 K (Table 2). Below about 20 K, the magnetic moment of Mn is slightly canted and thus yielding a small antiferromagnetic component in the [010] direction. The antiferromagnetic component is of A -type with alternating moments in the (200) plane with a magnitude of $0.42(5) \mu_B$ at 1.5 K. This

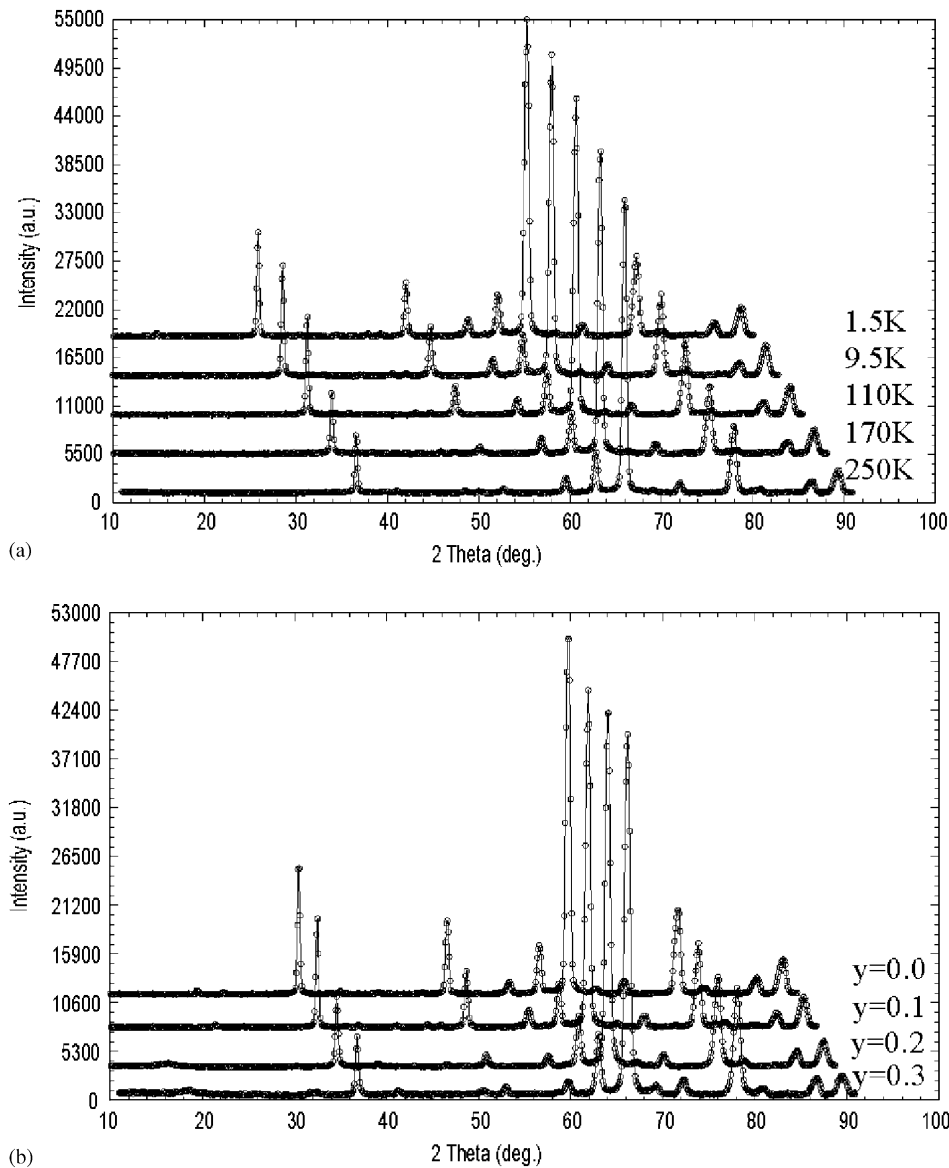


Fig. 3. (a) Neutron powder diffractograms for $\text{Nd}_{0.6}\text{Mg}_{0.1}\text{Sr}_{0.3}\text{MnO}_3$ at different temperatures. (b) Neutron powder diffractograms for all the samples at $T = 1.5$ K: for clarity, the curves in both (a) and (b) are shifted relative to each other both horizontally and vertically.

antiferromagnetic component generates some new intensities, easily observed on the 001 reflexion at $2\theta = 25.62^\circ$ (Fig. 4a). This is a forbidden reflexion in the crystallographic space group $Pnma$.

Below 50 K the Nd moment orders ferromagnetically along [001] and has a magnitude of $0.90(5)\mu_B$ at 1.5 K, i.e., in the same direction as the ferromagnetic component of the Mn moments, and thus contributing to the total ferromagnetic moment in the sample.

In the $\text{Nd}_{0.6}\text{Mg}_{0.1}\text{Sr}_{0.3}\text{MnO}_3$ sample, Mg substitutes only for Nd. The magnetic structure of $\text{Nd}_{0.6}\text{Mg}_{0.1}\text{Sr}_{0.3}\text{MnO}_3$ is similar to that of $\text{Nd}_{0.7}\text{Sr}_{0.3}\text{MnO}_3$, but the magnetic moments are smaller in magnitude and the T_C shifts towards lower temperature. As in the pristine compound, the Mn moment orders ferromagnetically

along the [001] direction below 170 K and has a magnitude of $3.12(4)\mu_B$ at 1.5 K. At temperatures below 20 K, the Mn moment is canted in the same way as in $\text{Nd}_{0.7}\text{Sr}_{0.3}\text{MnO}_3$ yielding an antiferromagnetic component along [010] with a magnitude of $0.43(5)\mu_B$ at 1.5 K.

The magnetic moment of neodymium orders ferromagnetically below 50 K in the same direction as the ferromagnetic component of Mn and has a magnitude of $0.79(6)\mu_B$ at 1.5 K.

3.3.2. $\text{Nd}_{0.6}\text{Mg}_{0.1}\text{Sr}_{0.3}\text{Mn}_{0.9}\text{Mg}_{0.1}\text{O}_3$ and $\text{Nd}_{0.6}\text{Mg}_{0.1}\text{Sr}_{0.3}\text{Mn}_{0.8}\text{Mg}_{0.2}\text{O}_3$

The Mn moment of the sample with $y = 0.2$, where Mg has substituted also for Mn, orders ferromagnetically along [001] below 250 K with a magnitude of

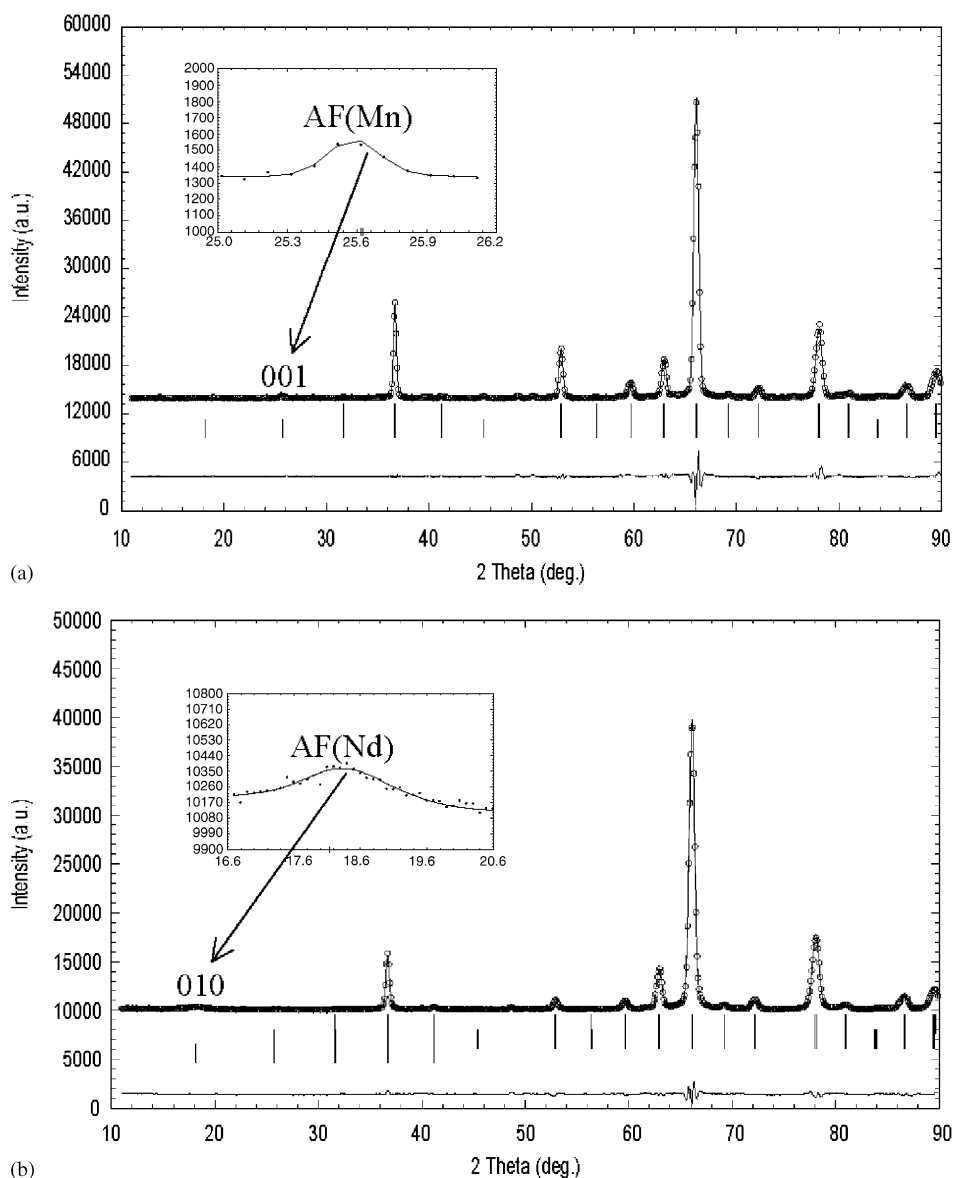


Fig. 4. (a) Rietveld refinement plot for $\text{Nd}_{0.6}\text{Mg}_{0.1}\text{Sr}_{0.3}\text{MnO}_3$ at 1.5 K: here and in Fig. 4(b) experimental points are marked with circles and the calculated profile with a solid line. The lower line is the difference between the experimental and calculated curves. The tick marks in the middle are reflection positions: the upper ticks are the reflection positions for the nuclear structure and the lower for the magnetic structure. (b) Rietveld refinement plot for $\text{Nd}_{0.6}\text{Mg}_{0.1}\text{Sr}_{0.3}\text{Mn}_{0.9}\text{Mg}_{0.1}\text{O}_3$ at 1.5 K.

$1.66(3)\mu_{\text{B}}$ at 1.5 K, thus showing a substantial decrease in magnitude compared to the two less substituted samples.

The Nd moment orders below 100 K but in contrast to the samples with Mg concentration, $y = 0.0$ and 0.1 , it orders in an antiferromagnetic way along the [100] and has a magnitude of $1.9(1)\mu_{\text{B}}$ at 1.5 K. The new intensity generated is broad and diffuse which can be seen on the crystallographically forbidden 010 reflexion in the angular range $17.57\text{--}18.92^\circ$ (Fig. 4b). This effect is a consequence of antiferromagnetic short range ordering of the Nd moment and was taken into account in the Rietveld treatment by using the Thompson–Cox–

Hastings pseudo-Voigt function with fixed half width parameters and refining the Lorentz size parameter. The value of the size parameter $\gamma = 1.7(3)$ corresponds to a correlation length of $\sim 51\text{ \AA}$ (correlation length = $89/\gamma$). A similar analysis on the ferromagnetic component of Mn moments for the same sample suggests that ferromagnetically ordered regions with a correlation length of 700 \AA appear in the sample below 250 K.

The substitution of more Mg ($y = 0.3$) in the Mn-site does not cause any significant change in the magnetic structure of the material. The magnitude of the Mn moment, however, is $1.65(4)\mu_{\text{B}}$, and that of the antiferromagnetic moment of Nd $1.6(1)\mu_{\text{B}}$ at 1.5 K

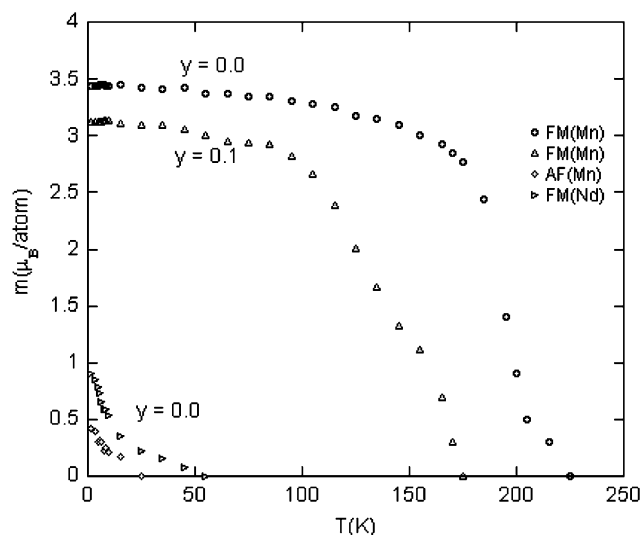


Fig. 5. The ferromagnetic moment of Mn vs. temperature obtained from the Rietveld analyses of neutron powder diffraction data of the samples with magnesium content $y = 0.0$ and $y = 0.1$. In addition, the low temperature antiferromagnetic component of the Mn moment and the ferromagnetic Nd moment for the $y = 0.0$ sample are indicated, respectively.

(Table 2). The ferromagnetic components of Mn in $\text{Nd}_{0.6}\text{Mg}_{0.1}\text{Sr}_{0.3}\text{Mn}_{0.8}\text{Mg}_{0.2}\text{O}_3$ and $\text{Nd}_{0.6}\text{Mg}_{0.1}\text{Sr}_{0.3}\text{Mn}_{0.9}\text{Mg}_{0.1}\text{O}_3$ vanish at about 250 K. The replacement of Mn by Mg ions in the *B*-site disrupts the double exchange and hinders long-range ferromagnetic order to establish in the samples. However, local ferromagnetic order within small regions (of size some hundred Å) establishes. In addition, a competition with antiferromagnetic superexchange interaction becomes significant. This causes an apparent spin glass-like maximum in the ZFC magnetization curves at low temperature (cf. Fig. 1). The fact that local ferromagnetic order appears at about 250 K in both the samples with $y = 0.2$ and 0.3 , may suggest that within the ferromagnetically ordered regions, the magnitude of the double exchange governs the transition temperature.

4. Discussion and conclusions

X-ray and neutron powder diffraction patterns show that both the pure and the magnesium substituted $\text{Nd}_{0.7}\text{Sr}_{0.3}\text{MnO}_3$ samples are single-phased with orthorhombic (*Pnma*, No. 62) symmetry. The nuclear structure remains orthorhombic within the temperature range 1.5–298 K. The two small extra peaks observed at 2θ angles 48–50° (Fig. 4a) cannot come from an impurity phase since they are not present in the 298 K data of the same sample from the diffractometer 3T2. We drew the conclusion that some neutrons have been scattered from the cryostat. A slight distortion in the structure and a decrease in the unit cell volume are

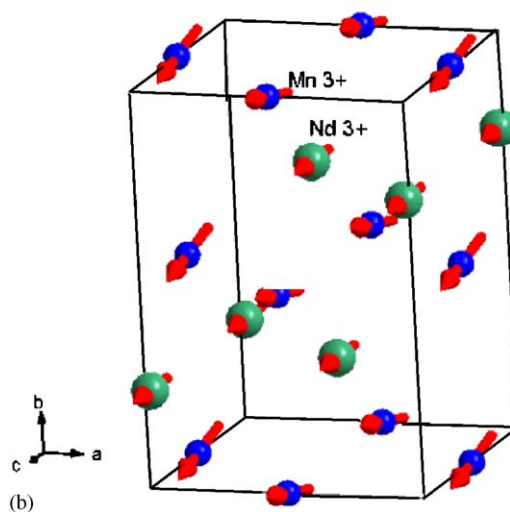
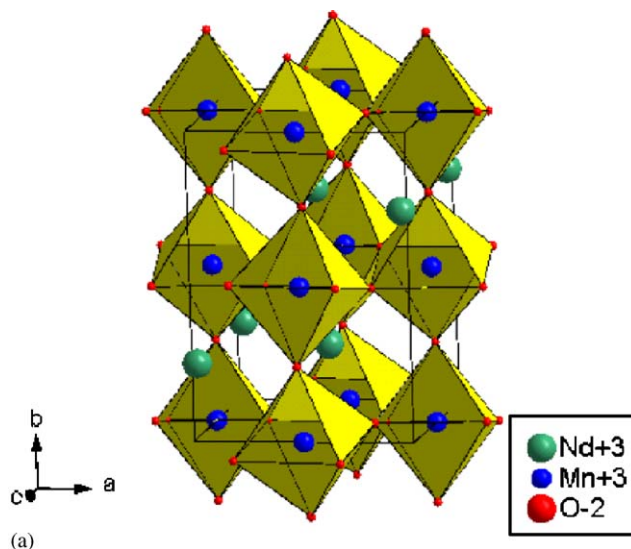


Fig. 6. The unit cell of $\text{Nd}_{0.6}\text{Mg}_{0.1}\text{Sr}_{0.3}\text{MnO}_3$: (a) Nuclear, and (b) magnetic structure at 1.5 K.

observed with respect to the pristine compound with increasing Mg substitution, but no significant change of the nuclear structure (Fig. 6a) is a representative structure) occurs due to the Mg-substitution [17].

There is a striking sensitivity of the transition temperature to the details of sample preparation and handling. For the pristine compound, $\text{Nd}_{0.7}\text{Sr}_{0.3}\text{MnO}_3$, T_C values ranging from 190–240 K have been reported in the literature, even the transition temperature of our current sample $T_C \approx 210$ K, deviates significantly from the earlier finding $T_C \approx 230$ K [16] for a sample that has been fabricated by the same recipe.

The magnetization and neutron powder diffraction experiments show that a long-range ferromagnetic order develops in the samples with low magnesium concentration $y = 0.0$ and 0.1 . With increasing magnesium substitution, the magnitude of the saturation magnetization decreases and T_C shifts toward lower

temperature from 210 K for $y = 0$ to 180 K for $y = 0.1$. The upturn of the saturation magnetization at lower temperatures for these two samples, illustrated in the inset of Fig. 2, is due to the ferromagnetic polarization of Nd moments as evidenced by the neutron powder diffraction results indicated in Fig. 5. At low temperatures (below 50 K) Nd is found to have a ferromagnetic moment (of order $1 \mu_B$ at 1.5 K) directed along [001]. A low-temperature polarization of the Nd ions in $\text{Nd}_{0.7}\text{Sr}_{0.3}\text{MnO}_3$ and $\text{Nd}_{0.7}\text{Ba}_{0.3}\text{MnO}_3$ has earlier been reported by Thomas et al. [19] and Fauth et al. [20], respectively.

For the samples with $\text{Mg} \geq 0.2$, long-range ferromagnetic order does not develop, but ordering of the Mn moments on short range occurs already at about 250 K. The magnetic moment of Mn is greatly reduced (about $1.6 \mu_B$ at 1.5 K) and decays unusually rapidly (almost linearly) towards zero at 250 K. Another feature of these two samples is that there occurs a local antiferromagnetic ordering of the Nd moments at low temperatures, in contrast to the long-range ferromagnetic polarization that occurs in the two samples of lower Mg concentration. The most significant difference between the $y = 0.0$ and 0.1 compared to the $y = 0.2$ and 0.3 is that Mg goes only to the Nd site in the first substituted compound, whereas, Mg also substitutes for Mn in the samples of higher Mg concentration ($y \geq 0.2$). This difference is apparently crucial for the magnetic properties and the difference can be associated to the fact that Mg substitution on the Mn site reduces drastically the $\text{Mn}^{3+}/\text{Mn}^{4+}$ ratio, which diminishes the influence of the DE interaction and favours AF superexchange.

Acknowledgments

The financial support from Sida/SAREC and the Swedish Research Council (VR) is gratefully acknowl-

edged. Many thanks are also due to the Centre Culturel Suédois in Paris for contribution to the French–Swedish collaboration.

References

- [1] C. Zener, *Phys. Rev.* 82 (1951) 403–405.
- [2] G.H. Jonker, J.H. Van Santen, *Physica* 16 (1950) 337–349.
- [3] P.W. Anderson, H. Hasegawa, *Phys. Rev.* 100 (1955) 675–681.
- [4] P.G. De Gennes, *Phys. Rev.* 118 (1960) 141–154.
- [5] R.M. Kuster, J. Singleton, D.A. Keen, R. Mcgreevy, W. Hayes, *Physica B* 155 (1989) 362–365.
- [6] R. Von Helmholt, J. Wecker, B. Holzapfel, L. Schultz, K. Samwer, *Phys. Rev. Lett.* 71 (1993) 2331–2333.
- [7] A. Maignan, B. Raveau, *Z. Phys. B* 102 (1997) 299–305.
- [8] H.L. Ju, C. Kwon, Qi Li, R.L. Greene, T. Venkatesan, *Appl. Phys. Lett.* 65 (1994) 2108–2110.
- [9] H.Y. Hwang, S.-W. Cheong, P.G. Radaelli, M. Marezio, B. Batlogg, *Phys. Rev. Lett.* 75 (1995) 914–917.
- [10] J. Fontcuberta, B. Martínez, A. Seffar, S. Pinol, J.L. García-Munoz, X. Obradors, *Phys. Rev. Lett.* 76 (1996) 1122–1125.
- [11] B. Raveau, C. Martin, A. Maignan, *J. Alloys Compounds* 275–277 (1998) 461–467.
- [12] S.B. Ogale, R. Shreekala, Ravi Bathe, S.K. Date, S.I. Patil, *Phys. Rev. B* 57 (1998) 7841–7845.
- [13] A. Anane, C. Dupas, K. Le Dang, J.-P. Renard, P. Veillet, A.M. De Leon Guevara, F. Millot, L. Pinsard, A. Revcolevschi, A.G.M. Jansen, *J. Magn. Magn. Mater.* 165 (1997) 377–379.
- [14] B. Raveau, A. Maignan, C. Martin, M. Hervieu, *Chem. Mater.* 10 (1998) 2641–2652.
- [15] Lide M. Rodriguez-Martinez, J.P. Attfield, *Phys. Rev. B* 54 (1996) R15622–R15625.
- [16] D.N.H. Nam, R. Mathieu, P. Nordblad, N.V. Khiem, N.X. Phuc, *J. Magn. Magn. Mater.* 226–230 (2001) 1340–1342.
- [17] M. Tseggai, R. Mathieu, P. Nordblad, R. Tellgren, L.V. Bau, D.N.H. Nam, N.X. Phuc, N.V. Khiem, G. André, F. Bourée, *J. Solid State Chem.* 177 (2004) 966–971.
- [18] J. Rodriguez-Carvajal, *Physica B* 192 (1993) 55–69.
- [19] R.-M. Thomas, V. Skumryev, J.M.D. Coey, S. Wirth, *J. Appl. Phys.* 85 (1999) 5384–5386.
- [20] F. Fauth, E. Suard, C. Martin, F. Millage, *Physica B* 241–243 (1998) 427–429.